

Biomedical Paper

Objective Method for Localization of Cortical Asymmetries Using Positron Emission Tomography to Aid Surgical Resection of Epileptic Foci

Otto Muzik, Ph.D., Diane C. Chugani, Ph.D., Chenggang Shen, M.S., Ednea A. da Silva, M.D., Jagdish Shah, M.D., Aashit Shah, M.D., Alexa Canady, M.D., Craig Watson, M.D., Ph.D., and Harry T. Chugani, M.D.

Departments of Radiology (O.M., D.C.C., C.S., H.T.C.), Pediatrics (D.C.C., H.T.C.), Neurology (E.A.D., J.S., A.S., C.W., H.T.C.), and Neurosurgery (A.C.), Children's Hospital of Michigan and Harper Hospital, Wayne State University School of Medicine, Detroit Medical Center, Detroit, Michigan

ABSTRACT We designed a semiautomated method for the objective detection of abnormal regions of tracer accumulation in the brain. The purpose of the present study was to examine the diagnostic performance of this method by applying it to patients with clinically intractable epilepsy of unilateral origin; they underwent [F-18] deoxyglucose positron emission tomography (PET) prior to surgical resection of epileptic foci. A semiautomated method for assessment of asymmetries in the brain cortex was developed that compares activity concentrations in homotopic cortical areas. When these differences exceeded a predefined threshold, the areas with lower activity were marked and 3-dimensional surface rendered images were created to guide placement of intracranial electrodes (ECoG) followed by surgical resection. The normal amount of asymmetry between small (0.5–0.7 cm²) homotopic cortical regions was determined as $5.9 \pm 4.0\%$ (mean \pm SD). The false-positive fraction was determined for cutoff thresholds of 1 SD (10%), 1.5 SD (12%), and 2 SD (15%) outside the mean and was found to be 89, 44, and 0%, respectively. The obtained sensitivity–specificity pairs for correct localization of epileptogenic lobes based on the ECoG results were best for the 15% threshold (80/94%, accuracy 0.90). This objective PET method allows the accurate determination of cortical asymmetries, and it proved to be highly efficient in guiding epilepsy surgery. *Comp Aid Surg* 74–82 (1998). ©1998 Wiley-Liss, Inc.

Key words: epileptic focus, image data analysis, positron emission tomography guided surgery, positron emission tomography, tracer asymmetries

INTRODUCTION

Previously applied methods for detection of abnormalities in positron emission tomography (PET) images employed either the definition of regions of interest (ROIs) configured according to structural anatomy^{7,11,12} or used geometrically

predetermined ROIs consisting of a number of image pixels.¹⁸ The location of these ROIs is determined by visual inspection of PET images or with reference to a coregistered or standard anatomical magnetic resonance imaging (MRI) scan.

Received March 25, 1998; accepted May 21, 1998.

Address correspondence/reprint requests to: Dr. Otto Muzik, Children's Hospital of Michigan PET Center, 3901 Beaubien Blvd., Detroit, MI 48201. E-mail: otto@pet.wayne.edu.

©1998 Wiley-Liss, Inc.

In contrast, clinical application of functional imaging studies frequently involves the assessment of an experienced reader in nuclear medicine, who visually examines the images for abnormal regions. This primarily involves the comparison of the right side of the brain to the left side to detect regions of asymmetry that represent either an increase or decrease in tracer accumulation, as judged by comparing asymmetry regions to the remainder of the image volume.

We developed a semiautomated method for the objective detection of cortical asymmetries that incorporates both anatomical and geometrical aspects. Individual activity concentrations in small, anatomically defined, homotopic cortical areas are automatically compared; when these differences exceeded a predefined threshold, areas with a decrease of tracer accumulation are marked. Our method has similarities to methods used previously for the objective quantification of the heart^{3,4} and the brain.^{6,10} To demonstrate the performance of our approach, we applied this method to [F-18] deoxyglucose (FDG) PET scans of normal subjects and patients with partial epilepsy. In addition, for epilepsy patients, results of intracranial electrocorticography (ECoG) during surgical resection of epileptic foci were compared to 3-dimensional (3-D) surface rendered regions of decreased tracer accumulation marked by the method. The EEG recordings from ECoG represented the independent reference method to which the PET abnormality was compared.

The study had the following objectives: to analyze, using receiver operator characteristics (ROC) curve analysis, the sensitivity and specificity of our method using FDG-PET in relation to ECoG and to display the PET-determined abnormality on 3-D surface rendered MRI images of the cortex to aid in presurgical planning of cortical resection.

MATERIALS AND METHODS

The protocol was reviewed and approved by the Institutional Review Board and the Radiation Safety Committee at the Children's Hospital of Michigan. Informed consent was a prerequisite for inclusion of normal controls in the study.

Control Population Group

Sixteen subjects with normal neurological examination were scanned as part of a separate PET project: four normal adults (three males, one female, age range 38.2–52.5 years, mean age 44.3 years) and 12 children (nine males, three females,

age range 3.4–16.10 years, mean age 10.3 years). All subjects were studied under fasting conditions (> 4 h). Furthermore, none of the subjects in this group was on medication.

Patient Population Group

Thirteen patients with intractable epilepsy underwent FDG-PET with surface electroencephalogram (EEG) monitoring. All of them were submitted to focal cortical resection guided by ECoG. This group included five adults (three males, two females, age range 20.4–46.9 years, mean age 31.5 years) and eight children (two males, six females, age range 1.3–17.6 years, mean age 6.2 years). Unilateral interictal FDG-PET abnormalities were observed in all subjects of this group.

PET

FDG was synthesized according to the method of Hamacher et al.⁵ Radiochemical purity, as assessed by thin-layer chromatography, was >95%. PET measurements were performed using the CTI/Siemens PET scanner EXACT HR (Hoffman Estates, IL), which allows simultaneous acquisition of 47 contiguous transaxial images with a slice thickness of 3.125 mm. The reconstructed image resolution obtained in the study was 5.5 ± 0.35 mm at full width at half maximum (FWHM) in plane and 6.0 ± 0.49 mm FWHM in the axial direction (reconstruction parameters: Hanning filter with 1.20 cycles/cm cutoff frequency).

Initially, a venous line was established for injection of FDG (5.3 MBq/kg equivalent to 0.143 mCi/kg). Scalp electrodes for the EEG were placed in all patients with intractable epilepsy according to the International 10-20 system to monitor electroencephalographic activity during the FDG uptake period (0–30 min postinjection). External stimuli were minimized by dimming the lights and discouraging interaction so that studies reflected the resting awake state. Blood samples were not collected from any of the patients. Sedation with intravenous nembutal or midazolam was used, if necessary, after the uptake period.

Thirty minutes after injection, the patient was positioned into the scanner. Using a low-laser beam system, the position of the patient's head was adjusted so that the imaging planes were parallel to the canthomeatal line. Subsequently, a static 20-min emission scan in 2-D mode was initiated, collecting approximately 1 million net true counts per plane. Calculated attenuation correction was performed on all images using the CTI/Siemens reconstruction software. The out-

line of the head was derived directly from the raw data by threshold fits to the sinograms according to Bergström et al.¹ If necessary, image sets were reformatted to correct for an asymmetric alignment of the brain.

PET Data Processing and Analysis

To allow an efficient analysis of PET data, a software package was written in IDL v. 5.0 (Interactive Data Language, RSI, Boulder, CO) and installed on a network of SUN Sparc/SGI workstations (SUN Microsystems Inc. and Silicon Graphics Inc., Mountain View, CA). The software package allows the objective definition of the location of regions of asymmetry on PET images, segmentation of MRI images to expose the brain cortex, and the display of the 3-D surface rendered MRI images together with the location of the PET abnormality. The 3-D surface rendering of PET and MRI images was performed on an SGI OCTANE workstation using the MEDx software package (Sensor Systems Inc, Sterling, VA).

Definition of Defect Location

To objectively define a regional cortical abnormality, a semiautomated analysis algorithm was applied to the transaxial PET images. This program was designed to sequentially process all supratentorial planes of a PET study. In each plane, the brain contour was automatically determined as a 25% isocontour (Fig. 1). Subsequently, the

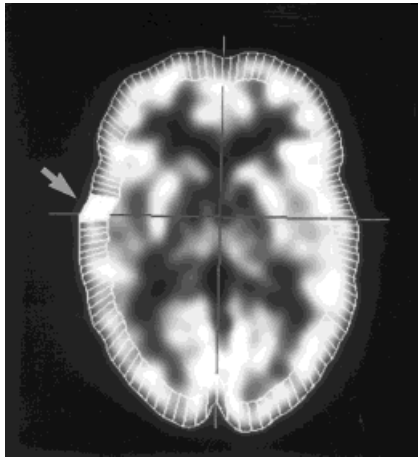


Fig. 1. Definition of 60 small homotopic regions in one transaxial plane of an FDG-PET scan. The user can interactively select the thickness of the cortical band. The arrow denotes regions where the asymmetry exceeded a predefined threshold. These regions were marked, allowing the reconstruction of the abnormality in 3-D surface rendered volumes.

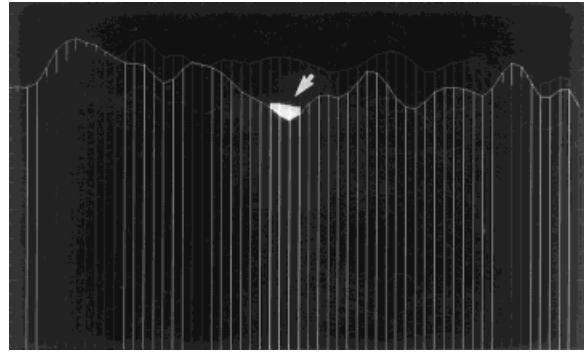


Fig. 2. Comparison of the left and right cortical profiles. Those cortical profile elements that fall below a user-specified threshold are determined and their position is marked in the original image plane (denoted by arrow, see also Fig. 1).

user defined a centerline separating the two hemispheres. This centerline was defined by selecting two points along this line, allowing a possible in-plane tilt of the brain to be taken into account. In addition, for each plane the brain centerpoint was defined as being located at the previously defined hemispheric centerline, as well as the thickness of the cortex (mostly 1.5–2 cm). Based on this information, the program automatically produced a second inner concentric line parallel to the previously defined outline. This second line depicted the inner border of the cortex. The data within this concentric band was then divided radially into 60 regions per hemisphere. Each individual region (0.5–0.7 cm² area) was bordered by the concentric band and radial lines originating from the centerpoint, creating a 3° wedge at the location of the cortex (Fig. 1). This resulted in 60 cortical data values for each hemisphere, which were displayed as a cortical profile (Fig. 2). Subsequently, the profiles for the left and right hemispheres were both overlaid so that the corresponding cortical values of both hemispheres could be found at the same ordinate. This was followed by the selection of a cutoff threshold on the side of the brain designated as normal. Because this method was designed to detect hypometabolic abnormalities in cortical brain regions, the chosen cutoff threshold represents the maximal asymmetry between corresponding profile elements (PE) considered within the normal range (H indicates higher, L lower):

$$\text{asymmetry} = \frac{[(PE_H - PE_L) / ((PE_H + PE_L) / 2)] \times 100\% \quad (1)}$$

If the asymmetry between the corresponding cortical profile elements at a certain ordinate exceeded the cutoff threshold, the lower profile element was marked. The positions of all marked profile elements were recorded and “painted” back into the original image set by setting them to the absolute maximum value found in the whole data volume (Fig. 1). In order to be considered as an abnormality, at least three adjacent profile elements had to be marked in two consecutive planes. Finally, a new static “marked” image file was created that included all 47 planes of the original frame.

MRI Data Processing

All patients with intractable epilepsy underwent a volumetric T1 MRI scan on a GE 1.5 Tesla Signa unit (GE Medical Systems, Milwaukee, WI) utilizing a spoiled gradient echo (SPGR) sequence. The 3-D SPGR sequence generated 124 continuous coronal sections of 1.5-mm thickness of the entire head, using a 35/5/1 (TR/TE/NEX) pulse sequence and a flip angle of 35°. The in-plane pixel resolution was 0.94 mm in a 256 × 256 matrix. MRI images were then transferred to CTI image format (256 × 256 × 124), and the cortical brain surface was exposed using an in-house written segmentation routine.

The segmentation routine works on the whole 3-D image volume and processes the data in three consecutive steps. Initially, a data classification is performed, segmenting out all pixels below a value of 7% (dura mater) and above a value of 70% (skull), of the maximal pixel value found in the whole image volume. The result is a first approximation of the brain gray matter surface, which is refined in the subsequent erosion–dilation operation. The erosion operation finds all surface pixels in the new volume and for each surface pixel sets all neighboring pixels to zero within a five-pixel cube (cube is centered by the surface pixel). The subsequent dilation operation recovers all surface pixels with the exception of those that represent thin connections into subdural space. In most cases, this cleanly separates the cortical surface from the skull. In those few cases where separation between cortex and skull could not be achieved, the user manually defined the surface of the cortex. In a last step, all connected components originating from one or more operator-defined seeds were determined and the background was set to zero, leaving a processed cortical brain surface.

Surface Rendering of PET and MRI Images

Matching of PET and MRI image volumes was performed using a multipurpose 3-D registration technique (MPITool) developed by the Max Planck Institute in Cologne, Germany.¹⁵ The coregistration method is highly interactive and is based on simultaneous alignment of PET-MRI contours that are exchanged in three orthogonal cuts through the brain. The advantage of the procedure is that it does not require external landmarks, nor is it affected by alterations in normal brain anatomy. Validation studies¹⁴ showed a high reproducibility, which was always much smaller than the PET image resolution, and an average displacement between PET and MRI images of less than 0.5 mm. The MRI data set was transferred to the PET center through the hospital computer network, converted to CTI image format, and the skull removed using the above-described segmentation software. The marked PET image volume was then coregistered to match the segmented MRI image volume, resulting in two matching 256 × 256 × 124 pixel data sets. To facilitate the anatomical localization of the epileptic defects and to relate the size and location to the whole brain surface, both newly created data sets were surface rendered using the Phong illumination model² provided by the MEDx software. In brief, given a 3-D volume and a surface constant value, the algorithm determines the vertices of all surface polygons and surface normals.⁹ This data is then used with the Phong shading algorithm to create a shaded surface of the brain cortex. The Phong shading algorithm proved to be superior to the standard Gouraud shading method due to the fact that surface normals are interpolated and the intensity function is computed for each pixel (being 3 times more computationally intensive than the Gouraud method). This results in a much lower dependency of the final surface on the underlying polygons, which usually constitute a grooved surface as a result of imperfection during the segmentation procedure. The surface constant values chosen were 25% for PET images and 5% for the segmented MRI images. The time to create the 3-D surface rendered images was about 30 s on an SGI OCTANE workstation with 256 MB of RAM. PET and MRI image sets were both 3-D surface rendered using identical viewing parameters, and the mark was localized on the PET surface using a maximum intensity projection. Finally, the mark was transferred to the MRI surface

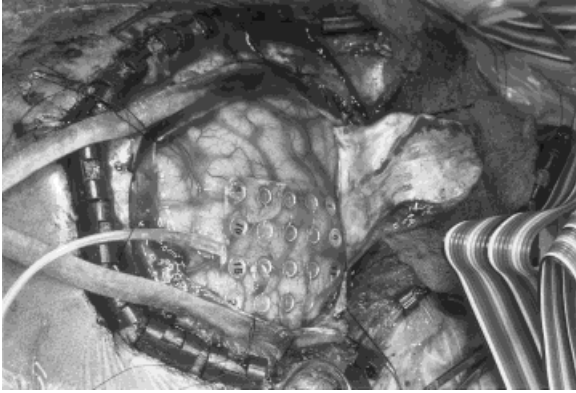


Fig. 3. Photograph taken during the resection of epileptic foci. Intracranial electrocorticography was performed prior to resection. The figure shows EEG electrodes positioned on the right temporal lobe of a patient.

using an IDL routine to delineate the affected sulci and gyri.

Epilepsy Surgery

All patients with intractable epilepsy underwent ECoG during surgical resection as part of their clinical treatment. A 4×5 electrode array was used to record from one to four positions on the cortical surface. The position(s) of the electrode array on the cortex was photographed (Fig. 3), and the presence of epileptiform activity for each electrode was recorded. The location of electrodes with epileptiform activity was then compared to the location of marked asymmetries on the FDG-PET images.

Statistical Analysis

The normal population was arbitrarily divided into two subgroups *N1* ($n = 8$) and *N2* ($n = 8$). All images showing the supratentorial cortex (usually 20–25 planes) obtained from group *N1* were used to determine parameters characterizing the normal asymmetry pattern. These parameters were the mean value and SD of asymmetries between homotopic cortical areas derived from all supratentorial planes of a study.

The obtained parameters were then applied to a combined group consisting of subjects from the epilepsy group and the control group *N2* to determine sensitivity (true positive decisions/number of patients with epilepsy), specificity (true negative decisions/number of control subjects), and accuracy of the proposed method. From these data, continuous ROC curves were generated from multiple sensitivity–specificity

pairs according to the method of Metz.¹³ To be recognized as a defect, at least three adjacent profile elements in two consecutive planes had to be marked. Sensitivity–specificity pairs were determined for cutoff thresholds of 1, 1.5, and 2 SD outside the mean difference value established in group *N1*.

In addition, the same cutoff thresholds were applied to the group of epilepsy patients, and the location of marked defects was correlated to the combined information from surface EEG and ECoG. The brain was divided into four lobe areas (temporal, frontal, parietal, occipital), and ECoG-EEG results for each lobe were compared to the area indicated as being asymmetric by FDG-PET. Again, sensitivity–specificity pairs were obtained for 1, 1.5, and 2 SD outside the normal mean differences of homotopic regions and a continuous ROC curve was generated.

RESULTS

Findings in Normal Control Scans

The asymmetry pattern derived from group *N1* showed a mean percentage difference of $5.9 \pm 4.0\%$, and this value was $5.7 \pm 4.1\%$ in group *N2* ($p = \text{NS}$). Applying a cutoff threshold of 1 SD (10%) outside the mean to group *N2*, all subjects showed at least one marked asymmetry. Raising the cutoff threshold to 1.5 SD (12%) outside the mean, three out of eight subjects still showed marked asymmetries. Finally, at a threshold of 2 SD (15%) outside the mean, none of the subjects in group *N2* showed any marked asymmetry.

Detection of Asymmetries in Combined Control–Epilepsy Group

The 13 epilepsy patients and 8 control subjects from group *N2* were combined into one group. Table 1 shows the obtained sensitivity–specificity pairs for cutoff thresholds of 10, 12, and 15%. The area under the ROC curve was 0.93, indicating an excellent overall reliability for the method (Fig. 4). The 10% threshold showed an unacceptable accuracy of 0.62 with only 11% specificity (equal to an 89% false-positive fraction), and the 12% threshold still showed only 66% specificity. Finally, the accuracy was highest for a threshold of 15% with no false-positive decision (specificity = 1.0) and a sensitivity for true asymmetries of 83%.

Localization of Asymmetries in Epilepsy Group

In our patient population with unilateral epilepsy, eight patients (66%) were diagnosed by ECoG to

Table 1. ROC Analysis of Data Obtained from Normal Controls and Epilepsy Patients Comparing Regional Asymmetry of Small Cortical Regions in FDG PET Images with Intracranial Electrocorticography

Threshold	ROC for Detection of PET Asymmetries in Normal Controls and Epilepsy Patients*			ROC for Correlating Asymmetries to EcoG Findings in Epilepsy Patients†		
	Sensitivity	Specificity	Accuracy	Sensitivity	Specificity	Accuracy
10%	1.0	0.11	0.62	1.0	0.75	0.85
12%	0.92	0.66	0.81	0.85	0.84	0.84
15%	0.83	1.0	0.90	0.80	0.94	0.89
Area under ROC curve		0.93		0.94		

* Normal controls represent true negative, epilepsy patients represent true positive.

† Lobes with positive EcoG represent true positive, all others represent true negative.

have epileptogenic tissue in only 1 lobe, three patients (25%) in 2 lobes, and two patients (17%) in 3 lobes. From a total of 52 lobes, 20 lobes were true positive and 32 lobes were true negative according to surface EEG-ECoG findings. Table 1 shows the obtained sensitivity–specificity pairs for cutoff thresholds of 10, 12, and 15%, resulting in an area under the ROC curve of 0.94 (Fig. 4). The accuracies were found to be high for all three thresholds (0.84–0.89), and the 15% threshold was the best. For this threshold, the sensitivity was 80% and the specificity was 94%, although the 10% threshold performed only slightly worse with 100% sensitivity and only 19% less specificity than the 15% threshold.

Visualization of PET-Defined Asymmetries on Cortical Surfaces

Figure 5 shows the 3-D surface rendered image of the cortex of one of the epilepsy patients. Su-

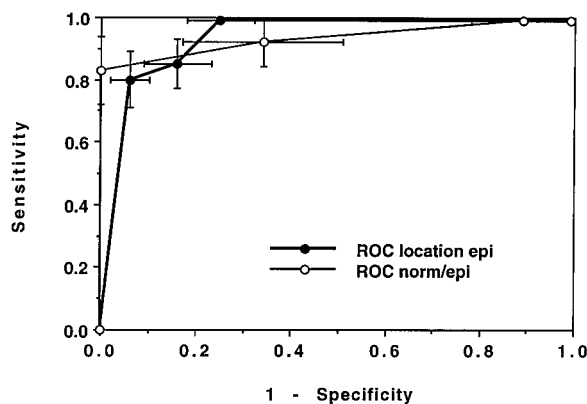


Fig. 4. The ROC curves obtained from sensitivity–specificity pairs at different asymmetry thresholds. Full circles represent the ROC curve determined when correlating PET-defined asymmetries with anatomical location of epileptic foci obtained by intracranial electrocorticography. The open circles represent the ROC curve for separating normal controls from epilepsy patients.

perimposed is the location and extent of the asymmetry as defined by PET, showing a mark on the lateral surface of the temporal lobe. Figure 6 shows the composition of a photograph showing the grid electrodes similar to Figure 3 (right posterolateral view) with the surface rendered image. The matching of both images was performed using Adobe Photoshop (Adobe Systems Inc.), based on anatomical landmarks recognizable on both images. The figure shows an excellent agreement between both modalities.

Surgical Outcome

All 13 patients with intractable epilepsy had focal cortical resection based on PET-guided placement of the ECoG grid. At present, the mean postsurgical follow-up time is 16 ± 5 months. Based on Engel's criteria, 6 out of 13 patients are seizure free, 5 patients have >75% seizure control improvement, and only 1 patient with non-lesional frontal lobe epilepsy has >50% seizure

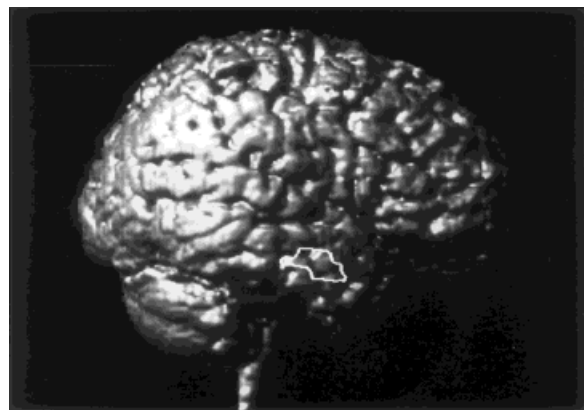


Fig. 5. A 3-D surface rendered display of the segmented MRI scan of an epilepsy patient. The border of the PET-defined defect is superimposed on the cortical surface for an improved assessment of the focus location.

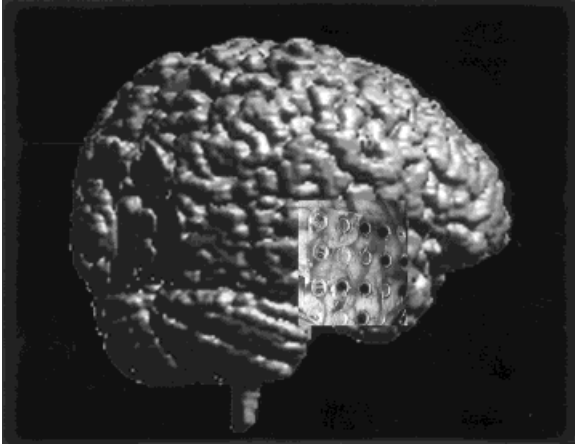


Fig. 6. A 3-D surface rendered display of the cortex (similar to Figure 5) showing the position of intracranial electrodes based on matching with a photograph taken during surgery. Electrodes that were active are marked with a dark spot.

control improvement. This patient was seizure free for 5 months after surgery but has a history of poor compliance with medication. Furthermore, this patient had a previous frontal lobe resection. Outcome is unknown in the remaining patient.

DISCUSSION

Evaluating a PET scan of the brain involves comparison of anatomical structures in both hemispheres to detect regions of asymmetry represented either as an increase or decrease of tracer accumulation. This is usually done by an expert observer who subjectively determines if the observed asymmetries represent true defects or normal anatomical variations of tracer distribution in the studied images. Methods that try to assess asymmetries in a more objective way employ the definition of ROIs in both hemispheres to obtain a numerical value for the activity concentrations in the particular ROIs.³ These values are then used to obtain an asymmetry index similar to that in eq. (1). Most often, ROIs are defined anatomically based on visual information derived directly from the PET scan or by reference to a coregistered MRI scan. Some groups also use circular ROIs with predetermined pixel numbers that are superimposed onto the images.¹⁸ These approaches work well when the observed defect affects a whole anatomical structure or at least a well-defined portion of it. However, representation of defects in the cerebral cortex seen in FDG-PET

images with disease are not necessarily confined to a well-defined anatomical structure, which makes the detection of these defects more difficult.

Our first objective was therefore to design an automated method for localization of cortical asymmetries in PET images that is not dependent on manual definition of anatomical structures and to validate this method with FDG-PET in normal controls and epilepsy patients. The method was evaluated using cutoff thresholds of asymmetry of 10, 12, and 15%, which correspond to 1, 1.5, and 2 SD above a preestablished normal mean. The results of the ROC curve analysis showed that a threshold of 2 SD (15%) above the normal mean for differences between homotopic cortical regions yields the best accuracy (89%) for localizing true asymmetries in the FDG-PET scans. This result agrees well with data presented by Theodore et al.¹⁸ who reported a threshold of 15% as being the most accurate for separating epileptogenic tissue from normal tissue in temporal lobe epilepsy. Using the 15% cutoff threshold, the sensitivity of the technique was 80% and the specificity was 94%. Thus, the method proved to be highly reliable in the detection of cortical asymmetries on FDG-PET scans.

The second objective of this study was to define the region of decreased (or increased) cortical metabolism on 3-D surface rendered MRI images of the individuals brains to define the exact region of abnormality, independently of predefined anatomically defined regions. This information has practical clinical relevance as shown previously.⁸ It allows the assessment of malformation in the region of functional abnormalities measured with PET. Sisodiya et al.¹⁷ showed that 3-D surface rendered MRI images are useful for detection of a cortical malformation that could not be detected on 2-D images. In addition, this information can be used in surgical planning when deciding on the positioning of the patient, the size of brain exposure, and the size and placement of subdural electrodes. Delineation of the PET abnormality on the MRI surface image also aids in detection of artifacts generated by this method. Due to the small region size (0.5–0.7 cm²) and the slight variation of the position of sulci in the two hemispheres, three adjacent elements in two consecutive planes had to fall below a specified threshold to be accepted as an asymmetry. Although this constraint significantly improved the performance of the method, it may not prevent the marking of a particularly deep sulcus.

The limitations of this study include the fact that intracranial electrodes were only placed on those lobes that were suspected to be abnormal by a combination of other modalities such as surface EEG, video monitoring, and neurological evaluation. This was necessary to minimize the invasiveness of the procedure. It is, however, conceivable that true asymmetries on FDG-PET images might have existed in lobes where no electrodes were placed and that were therefore assumed to be true negative. Furthermore, results of PET scanning are very much dependent on the applied tracer; it is well known that the tracer FDG shows a more extensive hypometabolic defect than other tracers used for determination of epileptic foci. For example, Savic et al.¹⁶ showed that the benzodiazepine receptor antagonist tracer flumazenil yields a more restrictive pattern of asymmetry than FDG and might have a better clinical performance when compared to ECoG. Nevertheless, our results show that cortical asymmetries in FDG-PET scans determined by our objective method correlate well with an independent measure of tissue abnormality.

The proposed method was specifically designed to detect asymmetries in the cortex; thus, it cannot be used for subcortical structures of the brain (e.g., the basal ganglia or the cerebellum). Furthermore, it is restricted to unilateral abnormalities, because it compares homotopic areas in both hemispheres. A potential source of error is an incorrect tilted alignment of the brain, resulting in comparison of cortical regions that do not represent homotopic areas. It is therefore essential for the accuracy of this method that, prior to its application, a correctly aligned data set is obtained, which can be easily achieved by reslicing the PET image volume.

CONCLUSION

In summary, the proposed method provides an operator-independent determination of cortical asymmetries, which proved to be highly accurate in localizing epileptic foci in FDG-PET scans. Further studies employing other PET tracers might result in an even better clinical performance and might significantly improve the success rate in epilepsy surgery.

ACKNOWLEDGMENTS

We would like to express our gratitude to Galina Rabkin, CNMT, Teresa Jones, CNMT, and Ben Lathrop, CNMT, for their expert technical assistance in performing the PET studies. We further

express our gratitude to Joel Ager, Ph.D., and James Janisse, M.S., from CHER for their statistical support. This work was partially supported by funding from NIH grant NS-34488.

REFERENCES

1. Bergstrom M, Litton J, Eriksson L, Bohm C and Blomqvist G (1982) Determination of object contour from projections for attenuation correction in cranial positron emission tomography. *J Comp Assist Tomogr* 6:365–372.
2. Foley J, van Dam A, Feiner S, Hughes J (1990) *Computer Graphics: Principles and Practise*. Reading, MA: Addison–Wesley, p 702.
3. Garcia E, Maddahi J, Berman D, Waxman A (1981) Space/time quantitation of thallium-201 myocardial scintigraphy. *J Nucl Med* 22:309–317.
4. Garcia E, VanTrain K, Maddahi J, Prigent F, Friedman J, Areeda J, Waxman A, Berman D (1985) Quantification of rotational thallium-201 myocardial tomography. *J Nucl Med* 26:17–26.
5. Hamacher K, Coennen HH, Stoecklin G (1986) Efficient stereospecific synthesis of no-carrier-added 2-[F-18]-fluoro-2-deoxy-d-glucose using aminopolyether supported nucleophilic substitution. *J Nucl Med* 27:235–238.
6. Harris G, Links J, Pearlson G, Camargo E (1991) Cortical circumferential profile of SPECT cerebral perfusion in Alzheimer's disease. *Psychiatry Res Neuroimag* 40:167–180.
7. Henry TR, Mazziotta JC, Engel J, Christenson PD, Zhang JX, Phelps ME, Kuhl DE (1990) Quantifying interictal metabolic activity in human temporal lobe epilepsy. *J Cerebr Blood Flow Metab* 10:748–757.
8. Levin D, Hu X, Kim K, Galhotra S, Pellizari C, Chen G, Beck R, Chen C, Cooper M, Mullah J (1989) The brain: Integrated three-dimensional display of MR and PET images. *Radiology* 172:783–789.
9. Lorenson C, Kline D (1987) "Marching Cubes": A high resolution 3D-surface construction algorithm. *Comp Graph* 21:163–169.
10. Maurer A, Siegel J, Comerota A, Morgan W, Johnson M (1990) SPECT quantification of cerebral ischemia before and after carotid endarterectomy. *J Nucl Med* 31:1412–1420.
11. Mazziotta JC, Phelps ME, Miller J, Kuhl DE (1981) Tomographic mapping of human cerebral metabolism: Normal unstimulated state. *Neurology* 31:503–516.
12. Mazziotta JC, Phelps ME, Plummer D, Schwab R, Halgren E (1983) Optimization and standardization of anatomical data in neurobehavioral investigations. *J Cerebr Blood Flow Metab* 3(suppl 1):S266–S268.
13. Metz CE (1978) Basic principles of ROC analysis. *Semin Nucl Med* 8:283–298.

14. Pietrzyk U, Herholz K, Fink G, Jacobs A, Mielke R, Slansky I, Wuerker M, Heiss WD (1994) An interactive technique for three-dimensional image reconstruction: Validation for PET, SPECT, MRI and CT brain studies. *J Nucl Med* 35:2011–2018.
15. Pietrzyk U, Herholz K, Heiss WD (1990) Three-dimensional alignment of functional and morphological tomograms. *J Comp Assist Tomog* 14:51–59.
16. Savic I, Ingvar M, Stone–Elander S (1993) Comparison of [C-11]flumazenil and [F-18]FDG as PET markers of epileptic foci. *J Neurol Neurosurg Psychiatry* 56:615–621.
17. Sisodiya SM, Stevens SJ, Fish DR, Free SL, Shorvon SD (1996) The demonstration of gyral abnormalities in patients with a cryptogenic partial epilepsy using three-dimensional MRI. *Arch Neurol* 53:23–34.
18. Theodore WH, Sato S, Kufta C, Balish MB, Bromfield EB, Leiderman DB (1992) Temporal lobectomy for uncontrolled seizures: The role of positron emission tomography. *Ann Neurol* 32:789–794.